



Hydrodynamics and particle transport associated with a submarine canyon off Blanes (Spain), NW Mediterranean Sea

Timothy C. Granata^{a,*}, Beatriz Vidondo^a, Carlos M. Duarte^a,
Maria Paola Satta^a, Marc Garcia^b

^a*Centre d'Estudis Avançats de Blanes, Camí Santa Bàrbara s/n, 17300 Blanes (Girona), Spain*

^b*Laboratori d'Enginyeria, Universitat Politècnica de Catalunya, C. Gran Capitán s/n, Modulo D1, 08039 Barcelona, Spain*

Received 22 August 1996; received in revised form 17 March 1997; accepted 5 November 1998

Abstract

Particle transport rates were observed to be higher in a submarine canyon in the NW Mediterranean Sea than in areas surrounding the canyon. Velocity and particle profiles were used to reconstruct a three-dimensional (2-layer) grid of the flow field and resulting particle transport. Canyon topography enhanced both horizontal and downward transport of particles in an anticyclonic flow region over the canyon. Particles were probably not produced locally within the canyon but were transported from shallow coastal areas. Inorganic particles accounted for 75% of the particle mass with organic particles accounting for the remainder. The total particle mass had an uneven spatial distribution with higher concentrations in the canyon and along the coast near the head of the canyon. Generally, organic particulate production was negative (indicating biological respiration) and negligible, however, positive production rates did occur near the coast coincident with an area of high total particle mass. The respiratory losses of the organic material were lowest in the canyon, coincident with downwelling regions of high mass transport, thus biological degradation of organic material was expected to be slow. The downward transport of total particulate material leaving the upper layer of canyon was $5 \times 10^7 \text{ kg d}^{-1}$, of which $1.2 \times 10^7 \text{ kg d}^{-1}$ was organic material. The near shore and central part of the canyon probably act as traps for suspended particles by transporting them deeper in the canyon where higher residence times resulting from reduced advection may facilitate their sedimentation to the bottom. © 1999 Elsevier Science Ltd. All rights reserved.

Keywords: Particle transport; NW Mediterranean Sea; Blanes canyon

*Corresponding author. Tel.: 0034 972 336101; fax: 0034 972 337 806.

1. Introduction

The shelf area of the NW Mediterranean features an indented topography, characterised by the presence of numerous submarine canyons. These canyons have been suggested to modify the mean flow (Masó et al., 1990; Masó and Tintoré, 1991; Alvarez et al., 1996), as well as to influence the sedimentation of particles exported from the coastal areas (Monaco et al., 1990). Recently, Olivar et al. (1998) and Sabatés and Olivar (1996) have also shown the importance of phytoplankton and larval fish distributions resulting from flow modification along this shelf. The most important fishery in the area is that of the deep water shrimp *Aristeus antennatus*, which is captured exclusively at depth ranges between 400 and 800 m in the canyon areas (Demestre and Martin, 1993). These prawns are detritivores, and their high population densities in the canyon areas support the contention that these areas should be important channels for the offshore transport of organic materials produced near shore (Monaco et al., 1990).

The Blanes canyon, located on the Spanish coast at 41°41'N and 2°48'E, is one of the most prominent canyons on the NW Mediterranean shelf. The major current in this region is the Catalan current which, originating off the French coast in the Gulf of Lions, flows SW along the coast. The coastal shelf off Blanes is a broad plain of approximately 200 m depth some 35 km offshore. The canyon, however, protrudes to within 18 km of the shoreline and thus bisects the path of the Catalan current. Simple considerations based on the conservation of momentum and vorticity suggest that velocities in the canyon should be reduced and that downwelling should occur in the upper layer as a result of vortex stretching. Past studies have indeed shown that the canyon has a pronounced affect on the vorticity of the flow field, causing the flow to meander with an anticyclonic rotation upstream of the canyon and cyclonic rotation over the canyon (Masó et al., 1990; Masó and Tintoré, 1991). However, Rojas et al. (1995) have shown this typical flow pattern can be altered with flow reversing in the upper layer after the development of a strong pycnocline in the spring.

Generally, currents in submarine canyons have been shown to enhance particle transport as a result of canyon topography (Inman et al., 1976; Hickey et al., 1986; Durrieu de Madron, 1994). Canyons may act as collectors for falling particles transported into them, provided that deep horizontal flows are weakened and downwelling flow is strong. The major sources of particles in the Blanes canyon are terrestrial and marine. Terrestrial particle transport is probably associated with episodic loading from the nearby Tordera River and from run-off of ephemeral streams along the steep, coastal valleys. Marine particles are most likely sand and biogenic material (i.e. plankton and detritus) transported and produced locally. The working hypothesis of this study was that the canyon is a sink for particles within the area.

2. Methods

The study was conducted over the submarine canyon off Blanes, Spain, in the NW basin of the Mediterranean Sea. A grid of 8 transects consisting of 45 stations was

sampled in 4 days by the R/V *Hesperides* in June of 1993. The horizontal dimensions of the grid were roughly 80 km × 80 km with an average distance of 8 km between stations. Physical properties of the water column at each station were determined by profiling with a Mark V CTD. The horizontal resolution of the CTD data and water samples was on average 8 km, and down to 4 km in the canyon. Raw CTD data, which had a vertical resolution of about 10 cm, were corrected for spurious points and averaged to 1 m bins. Buoyancy frequency was determined from density profiles and density was calculated using standard algorithms (Fofonoff and Millard, 1981). Water samples were taken at discrete depths from a Rosette fitted with Niskin bottles. Horizontal velocity (u, v) profiles from 17 to 350 m were measured with a 150 kHz ADCP (RD Instruments) mounted in mid-hull of the ship. Raw ADCP data were sampled every 1.23 s over 8 m bins. The bridge gyro was used to correct the navigation (GPS) referenced data and bottom tracking referenced data. Bottom tracking was used for depths < 300 m while at deeper stations velocities were referenced to the average speed between 50 and 170 m. After correcting for navigational errors, which included abrupt changes in ship direction, and for statistical outliers, profiles were averaged to 5 min bins.

To assess flows and particle transport in the canyon, data were objectively mapped to a standardised grid centred on the canyon and with a horizontal resolution of 7.5 km between points. Fig. 1 shows the bathymetry of the canyon area with the locations of the sampling stations and the standardised grid points.

The depth integrated flow per unit length and unit mass, M , was calculated at each grid point as:

$$M_{x_{ij}} = \int_{z^-}^z u_{ij} dz; \quad M_{y_{ij}} = \int_{z^-}^z v_{ij} dz, \quad (1)$$

where dz is the depth increment (8 m), $u_{i,j}$ and $v_{i,j}$ are the east-west and north-south velocity components, respectively for transect i and station j . Flow was calculated in an upper layer from 17 to 100 m (or to the bottom if < 100 m), and in a lower layer, from 100 to 200 m (or to the bottom if < 200 m). Assuming incompressibility and no flow through the upper surface, continuity of the flow was invoked in control volumes to estimate vertical flows across the bottom of each layer such that

$$\left(\frac{\partial M_x}{\partial x} + \frac{\partial M_y}{\partial y} - w_z \right) \delta x \delta y = 0, \quad (2)$$

where the sides of the control volume are $\delta x, \delta y = 7.5$ km. Based on this notation, positive values represented upwelling conditions and negative values represented downwelling conditions.

We chose the control volume approach, using the divergence operator in Eq. (2), because it is very relevant to the study of vertical fluxes of particles (Dickey and Siegel, 1988). As a test of the validity of continuity, vertical velocities were assessed in control volumes along the coast for stations where the total depth was < 200 m. Since Eq. (2) was integrated from the near surface to 100 m for the upper layer and from 100 to 200 m for the lower layer, vertical velocities should be zero where the depth is less than

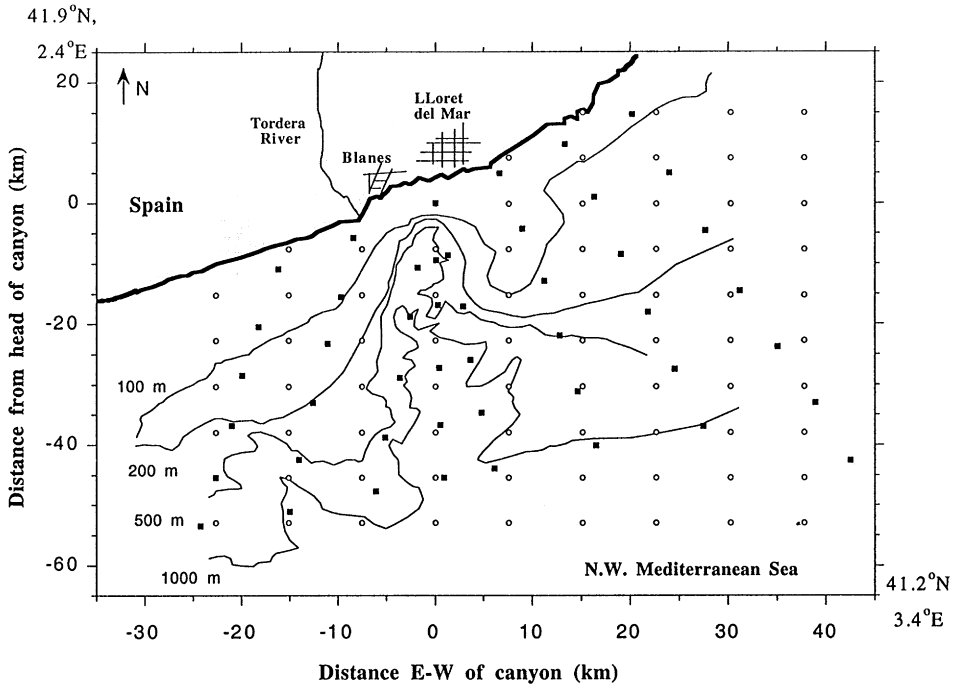


Fig. 1. A map of the study site showing the bathymetry, the sampling stations (filled squares), and the standardised grid points (open circles). N-S and E-W distances are in km's relative to the head of the canyon.

the limits of integration since there can be no flow through the bottom. Control volumes for the upper layer had near zero values (an rms of 1% of the rms value for entire grid), while those in the lower layer had rms values $< 10\%$ of rms velocity for the entire grid. So, the assumption of flow continuity seems valid. The uncertainties in vertical flow for the whole grid were determined as the standard error in w_z was based on the method of Topping (1971):

$$(w_{err})^2 = \left(\frac{\partial w_z}{\partial \Delta M_x} \right)^2 \alpha_{\Delta M_x}^2 + \left(\frac{\partial w_z}{\partial \Delta M_y} \right)^2 \alpha_{\Delta M_y}^2, \quad (3)$$

where w_{err} is the error associated with differencing the horizontal divergence operator in Eq. (2), $\alpha^2 = \sigma^2/N$, σ is the standard deviation and N is the number of points. The errors associated with the δy and δy terms in Eq. (2) are zero since $\alpha^2 = 0$ for the standard grid. As an independent check of vertical velocity, w_z was estimated following Leach (1987) and Tintoré et al., (1991) using the Omega equation:

$$N^2 \nabla_h w_z + f^2 \frac{\partial^2 w_z}{\partial z^2} = 2 \nabla_h \left(\frac{g}{\rho} \left[\frac{\partial u}{\partial x} \frac{\partial p_z}{\partial x} + \frac{\partial v}{\partial x} \frac{\partial p_z}{\partial y}, \frac{\partial u}{\partial y} \frac{\partial p_z}{\partial x} + \frac{\partial v}{\partial y} \frac{\partial p_z}{\partial y} \right] \right), \quad (4)$$

where N is the buoyancy frequency (s^{-1}), f is the inertial frequency (s^{-1}) which varied $< 1\%$ over the grid, g is the gravitational constant (9.8 m s^{-2}), and ρ_z is the density at depth z . The vertical velocity across the surface at depth z is w_z and was calculated assuming that the vertical gradients in w_z across the 100 m surface were small, $N^2 \nabla_h w_z \gg f^2 \partial^2 w_z / \partial z^2$. This simplified version of Eq. (4) was then solved for w_z at the bottom surface of each new grid point using a relaxation method (Hockney and Eastwood, 1994) where the boundary conditions were no flow through the coast and no change in w_z across the horizontal boundaries, i.e. $\partial w_z / \partial x, \partial w_z / \partial y = 0$. Residual errors in the relaxation scheme were $< 2\%$. Numerical integration by a quadratic method (Fletcher, 1984) gave similar results but a somewhat larger error. Finally, the assumption of small vertical changes in w_z was substantiated by solving Eq. (4) for w 's on surfaces $\pm 8 \text{ m}$ of z and observing that all velocities were within 10% of w_z values. While vertical velocities based on the Omega equation are probably more accurate than those calculated by continuity (Leach, 1987), the draw back to using the Omega equation is that the boundaries, and thus the horizontal dimensions, of the grid are drastically reduced as a result of the differencing scheme. Consequently, continuity (i.e. divergence from Eq. (2)) was used to estimate vertical fluxes of particles over the entire grid.

To visualise flow over the entire coastal region, a streamline function was defined as

$$\psi = \iint_{yz} u \, dz \, dy - \iint_{xz} v \, dz \, dx, \quad (5)$$

where the flow extends from the surface to the bottom. Since at many of the deeper stations (30% of the grid) velocity data were unavailable, velocities were assumed to decay to zero exponentially toward the bottom. Surface velocities (0–17 m) were set equal to those at 17 m. Eq. (5) differs from Eq. (2) in that velocities are integrated over the entire water column and thus, only horizontal flow is possible.

Seston was sampled from Rosette casts. Seston mass, C , ($> 0.7 \mu\text{m}$) was calculated as the dry weight (24 h at 80°C) of particles retained on saturated Whatman GF/F filters. Organic matter was estimated from the mass lost after ignition at 600°C for 24 h, the weight of the remaining material representing the mass of inorganic material such that $C_{org} = C - C_{inorg}$. The net mass of organic material produced or lost (C_{net}) was estimated from the net production as, $P_{net} \times 1 \text{ day}$ and added to the mass of material in the layer ($C_{total} = C + C_{net}$). P_{net} was estimated from oxygen evolution. Water samples were filtered through a $243 \mu\text{m}$ mesh to remove macrozooplankton, and carefully siphoned into 125 ml narrow-mouth Winkler bottles. Initial oxygen concentrations were immediately determined on five replicate bottles and incubations of 'dark' and 'light' bottles were carried out using five replicates each. Bottles were placed in an incubator for 20–24 h at ambient sea temperature. The relatively long incubation times, similar to those used for plankton-poor waters (Williams and Jenkinson, 1982), were necessary to obtain reliable estimates of oxygen changes in these sparse plankton communities. Dissolved oxygen concentrations were analysed using a Winkler titration, with automatic potentiometric end-point detection based on changes in Eh potential (Oudot et al., 1988) determined with a Metrohm-682

Autotitrator. The coefficient of variation for replicated estimates of dissolved oxygen concentration was 0.5%. P_{net} ($\mu\text{mol O}_2 \text{ m}^{-3} \text{ d}^{-1}$) was then calculated from the rate of change in oxygen concentration in ‘light’ bottles, corrected for night time respiration using the oxygen consumption in ‘dark’ bottles. The estimates of net production, based on O_2 production, were converted to carbon-based net production using a photosynthetic quotient of 1.2 (Vollenweider, 1974).

3. Results

Density distributions (σ_t) at 100 m (Fig. 2a), plotted on streamlines integrated over the entire water column, show that the horizontal density field in the surface layer parallels the flow field. Flow shows an anticyclonic pattern over the canyon and a cyclonic pattern offshore of the canyon. The dashed lines in the Fig. 2 represents the boundary between eastward and westward flow, based on the zero value of the depth integrated E–W velocity, $M_x = 0$, in the 2 layers. Eastward flow is predominant along the coast, to the north of the line, and westward flow to the south of the line. Two density minima were located in the canyon region coincident with the anticyclonic circulation (marked by A’s in Fig. 2). The highest densities were located offshore and near the area of the cyclonic flow, which has been marked with a C. The density on the 200 m surface also paralleled streamlines and so was similar to that in the upper layer,

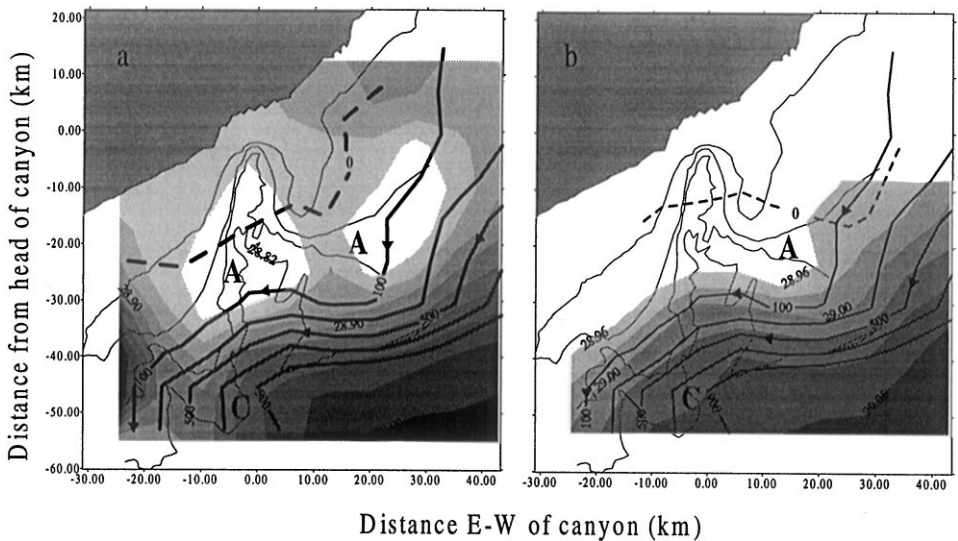


Fig. 2. Density distributions, σ_t (shaded, kg m^{-3}) for the: (a) upper layer; and (b) lower layer. The dashed line indicates $M_x = 0$ in each layer with flows south of the line moving to the west and those north of the line moving to the east. Streamlines ($10^3 \text{ m}^3 \text{ s}^{-1}$), based on Eq. (5), are represented by bold lines and bathymetry by thin lines. Anticyclonic regions of circulation are noted with an A and cyclonic centres with a C.

with the exception that the density maximum, associated with the cyclonic flow into the canyon, was displayed westward and shoreward. The SW flow veered onshore upstream of the canyon, and offshore after passing the canyon. Although not plotted, salinity in both layers mimicked density patterns over the grid, exhibiting 2 local minima of 37.2 ppt in the canyon (location A's) and a maximum of 37.8 ppt offshore (location C).

Figs. 3a–c, illustrate vertical sections of density and velocity perpendicular to the coast, progressing from the western extreme of the canyon (Fig. 3a, $x = -22.5$ km), to the centre of the canyon (Fig. 3b, $x = 0$ km), and to the east of the canyon (3c, $x = 30$ km). Near the coast, flow moved eastward, starting as a narrow jet in the shallow depths west of the canyon (Fig. 3a), then deepened with a reduction in velocity in the canyon (Fig. 3b), and then accelerated to a narrow jet leaving the canyon as the bottom shallowed to the east (Fig. 3c). Offshore flow was westward varying between 10 km (Fig. 3a) to 30 km (Fig. 3c) from the head of the canyon. The flow reversal in the central portion of the canyon created a high shear region between 10 and 30 km from the canyon head (Fig. 3b). This high shear zone extended to > 200 m depth and corresponded to the region of anticyclonic circulation in Fig. 2. In the upper 100 m of the canyon, density surfaces downwelled between 10 and 30 km (Fig. 3b), coincident

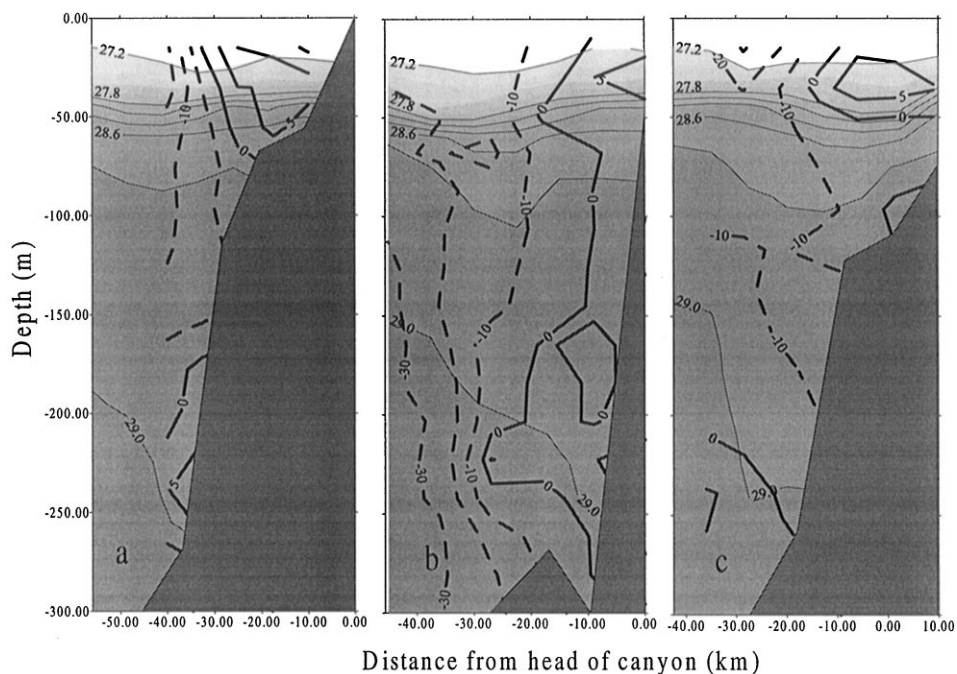


Fig. 3. Vertical distributions of density, σ_t (kg m^{-3}) and the E–W velocities (cm s^{-1}) for three transects perpendicular to the coast. The left most plot (a) is the western most transect, the middle plot (b) is centred on the canyon, and plot on the right (c) is the eastern most transect. Positive velocities are along the coast (solid lines) and to the east while negative velocities (dashed lines) are offshore and to the west.

with the anticyclonic feature. In contrast, the deeper 29 kg m^{-3} density surface was tilted upward. This compression of the water column indicates negative vorticity changes (anticyclonic) in the canyon between 10 and 30 km from the head of the canyon.

Organic particulate material was linearly related ($r^2 = 0.89$) to the Seston mass, and thus also related to inorganic material (Fig. 4). The concentration of organic material was 25% of the particulate material by weight, thus the inorganic material comprised nearly 75% of the particle mass. Because of the proximity of gross production and respiration in the biogenic layer, net planktonic metabolism was quite small with C_{net} , on average, about 0.1% of the total particulate matter.

Concentrations of total particulate material were non-uniformly distributed over the study area. The highest concentrations of total particulate material were in the eastern portion of the canyon, in the area of the anticyclonic flow (Fig. 5a). A secondary particle high occurred at the head of the canyon at the coast. Low concentrations of total particulate matter in the canyon area were found offshore and at the mouth of the canyon, near the centre of the cyclonic flow. Near zero concentrations were found NE of the canyon along the coast, following the boundary of the eastward current. Like the distribution of total particulate matter in Fig. 5a, the highest concentrations of organic and inorganic materials were east of the canyon and within a secondary maximum at the head of the canyon (not shown). Net production of particles, C_{net} , was low and negative in nearly all stations, indicating minor net losses of organic material to respiration. The exception was at the head of the canyon, near the coast, where positive values of C_{net} indicated a minor production event which coincided with the location of the peak in C_{total} near the coast. The highest loss rates occurred far east of the canyon and offshore of the canyon.

At the base of the 100 m surface, vertical velocities calculated from the continuity equation using the standard grid showed downward peaks of 40 m d^{-1} in the canyon

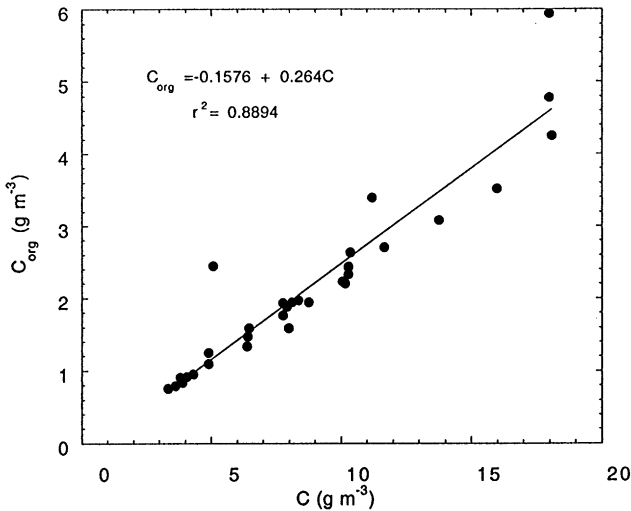


Fig. 4. A linear regression of organic particulate material on particulate material (Seston).

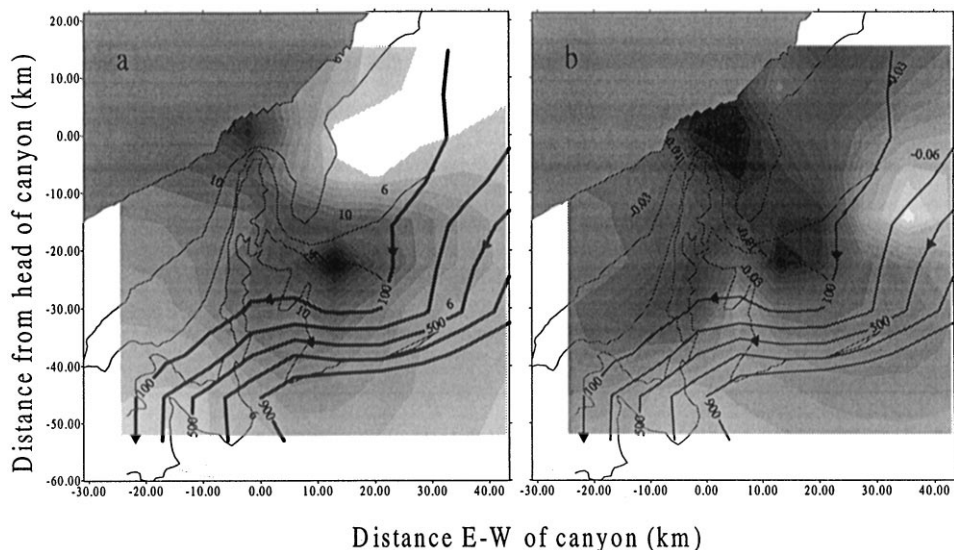


Fig. 5. Streamlines (bold lines) and bathymetry (thin lines) plotted on contours of: (a) C_{total} (shaded, g m^{-3}); and (b) C_{net} (shaded, g m^{-3}).

in the areas where the density minima occurred (at A), which was also the location where total particulate material was highest (Fig. 6a). The velocities in the lower layer were nearly double those in the upper layer (not shown). Upwelling velocities occurred at the mouth of the canyon, coincident with the density maximum and the lower particle loads, and had values of 80 m d^{-1} in the upper layer. The errors associated with the vertical velocities calculated from the continuity equation were larger in the lower layer than in the upper layer (Table 1), indicating a higher variability in the lower layer. The independent estimate of vertical velocity made at 100 m using the Omega equation showed a similar spatial distribution of downwelling and upwelling features; however, these features do not exactly coincide because of gridding differences inherent in the two methods. Although the directions of the vertical velocities are similar, their magnitudes are not, with peak velocities for the Omega equation lower by 5–10 fold (Fig. 6b).

4. Discussion

The observation of a SW current flowing along the continental slope is in agreement with previous descriptions of general circulation in the NW Mediterranean Sea (e.g. see Font et al., 1988; Castellón et al., 1990; Millot, 1990). Eddies and meandering currents appear to be common features along the Mediterranean shelf break as evidenced by satellite imagery of local surface flows (Tintoré et al., 1990). Current meandering has been related to topography of the NW Mediterranean canyons (Masó

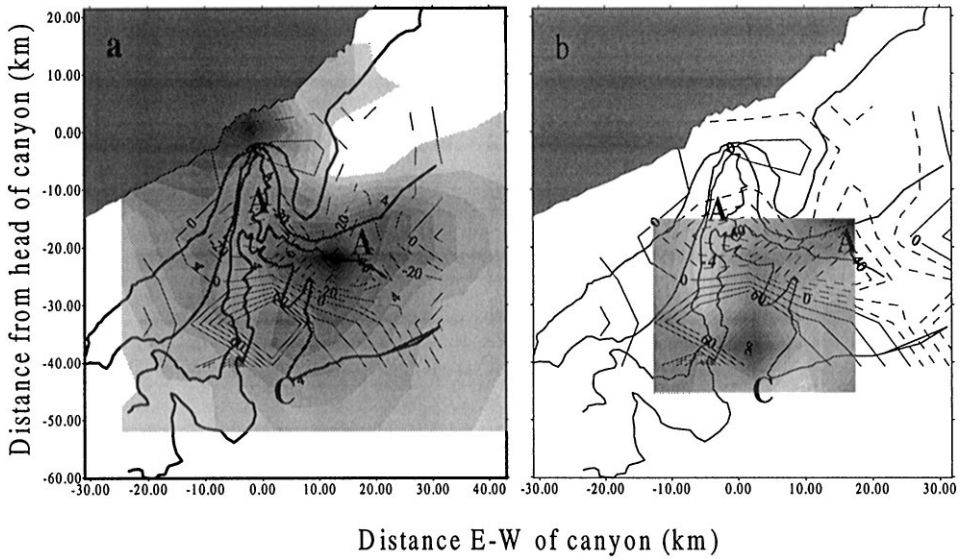


Fig. 6. Contours of: (a) total particle concentration, C_{total} (shaded, g m^{-3}) and vertical velocities at 100 m (m d^{-1}) calculated from Eq. (2) (lines); and (b) vertical velocities at 100 m calculated from the Omega equation (shaded, m d^{-1}) and vertical velocities calculated from Eq. (2) (lines). Upward velocities are positive (solid lines) and downward velocities are negative (dashed lines) for the continuity equation (Eq. (2)), while for the Omega equation positive (negative) velocities are dark (light) shades and magnitudes are italicised.

Table 1

The percentage of the standard error in vertical velocity, w_z , over the whole grid and within the canyon area

Location	Grid points	Standard error
Whole grid	81	5%
Canyon, upper layer, 100 m	32	15%
Canyon, lower layer, 200 m	25	41%

et al., 1990; Masó and Tintoré, 1991). The evolution of such meanders and eddies may be linked to flow modifications manifest by changes in current direction and/or acceleration over abrupt topographic features (Carnevale et al., 1989; Alvarez et al., 1996). For the Blanes canyon, conventional arguments for the conservation of potential vorticity suggest that the flow should acquire a negative relative vorticity upstream (the resulting decrease in absolute vorticity would be offset by the decrease in depth) and then gain positive relative vorticity as the water moves over the deeper bottom in the canyon. We did observe this type of canyon steering of the current. In

addition, we observed a change in flow direction between coastal and offshore waters with coastal waters flowing to the east and offshore waters flowing to the SW. This created a region of high horizontal shear which was augmented by a reduction of eastward velocities as coastal flow entered the canyon. These combined effects produced an extensive region of anticyclonic circulation from the eastern to the western rim of the canyon.

The highest flows in the coastal region were in the offshore jet. Total flow in the canyon can be assessed for a volume bounded by the canyon rims, $x = \pm 7.5$ km, the coast, and the mouth of the canyon offshore at $y = -52.5$ km. For this region of the canyon, the cross canyon flow was 0.74 Sv westward ($1 \text{ Sv} = 10^6 \text{ m}^3 \text{ s}^{-1}$), while the along canyon flow, southward out of the mouth of the canyon, was about half, at 0.46 Sv. The coastal flow was eastward at 0.039 Sv, 5% of the offshore jet. In terms of particle transport, the offshore jet transported $8.3 \times 10^8 \text{ kg d}^{-1}$ while the coastal current contributed only $0.6 \times 10^8 \text{ kg d}^{-1}$. When the control volume was extended to the eastern rim of the canyon to include stations with the highest downwelling velocities and particle concentrations, the amount of material entering the canyon was $5 \times 10^7 \text{ kg d}^{-1}$, of which $1.2 \times 10^7 \text{ kg d}^{-1}$ was organic material. In the upwelling zones, including the canyon mouth, total transport was $2 \times 10^7 \text{ kg d}^{-1}$, with $0.5 \times 10^7 \text{ kg d}^{-1}$ being organic. While the magnitudes of vertical transport may be overestimated, as indicated by the lower velocities using the Omega equation, the ratio of downwelling to upwelling should be correct. For our purposes, the divergence method and the Omega equation are in reasonable agreement. For more complex flows where velocities do not vary smoothly and for unsteady flows, however, the Omega equation may be more accurate since it includes information on the horizontal structure of the density field and of the gradients in vertical velocity field, both of which are averaged out using the continuity approach. Regardless of which method we use, we show that the main effect of the canyon would be to enhance downward transport within the canyon.

A modelling study of canyon flow by Klinck (1996) included a strongly stratified, downwelling case (i.e. coast to the right of the offshore current and strong stratification), conditions which mirror those in this study. The results of model were comparable to our results in that: (1) the largest downwelling velocities were located on the upstream rim of the canyon, (on order 90 m d^{-1}) and (2) offshore flow veered into the canyon with a downwelling of the density surface at depth. There were also dissimilarities such as modelled upwelling on the downstream side of the canyon, which was not evident in this study. The same model also demonstrated that the cross shelf transport was smaller than the along shore transport, and that as stratification increased, canyon downwelling was reduced by a factor of three and cross shelf transport by one-half. This has interesting consequences for partitioning of transport. For example, vertical transport of terrestrial particles into the canyon may be lower during conditions of high river flow since the sediment loads in rivers coincide with strong stratification resulting from lower surface salinity. Sedimented particles would presumably have maximal transport during storms that resuspend sediments and reduce stratification. Blooms of biogenic particles usually occur after the onset of stratification and thus would be downwelled at a slower rate for stratified

conditions. Further, daily respiration was low in most of the study area, so organic particles were probably not lost to respiration before they were able to sediment to the bottom.

Inorganic particles dominated the total particle mass in this study, consistent with previous reports of particle flux for other canyons in the NW Mediterranean (Monaco et al., 1990). Although the source of the inorganic particles was not known, there may be significant terrestrial inputs from the Tordera River which is near the head of the canyon where maxima in C_{inorg} , C_{org} and P_{net} occurred. Although the river may have played some role in episodic deposition of particulate material along the coast, it had low flow discharge during and before this study and, thus, probably did not directly contribute to coastal transport. The other region of high C_{inorg} and C_{org} was within the downwelling zone of the anticyclonic circulation. The anticyclonic vortex over the canyon may have concentrated particles in the core of the eddy where they were subsequently downwelled. This scenario is appealing since downwelling velocities were highest where particle loads were highest, in the anticyclonic flow over the canyon. The upwelling feature at the mouth of the canyon could aid in the suspension of particles by reducing sinking rate losses. Upwelling could also increase the upward flux of nutrients through the base of the euphotic zone, though in this case we might expect higher values of C_{net} (positive) and C_{total} , unless production were balanced by losses. Since calculations of net production were limited to the upper 200 m, they were representative of production in the euphotic zone, and thus, were probably related to phytoplankton production. The tight linear coupling between C_{org} and C_{total} suggests that biological processes, as well as physical transport processes, affected particle distributions over the canyon. Net production of organic matter was negative at most stations which may be a result of downwelling of nutrient depleted water below the pycnocline. Time series examination of coastal planktonic communities in the NW Mediterranean Sea has shown a close balance between gross production and respiration, with a tendency towards net heterotrophy (Satta et al., 1996). For the data examined here, integrated net community metabolism in both layers, $\int_z P_{net} dz$ ($z \leq 200$ m), showed a close coupling between production and consumption processes, with only a marginal ($-9 \text{ g m}^2 \text{ d}^{-1}$ on average) tendency for net heterotrophy. Hence, the close balance between production and consumption observed in a coastal area of the NW Mediterranean Sea (Satta et al., 1996) appears to reflect a balance even on the mesoscale. The minor contribution of biological production to the downward particle flux has also been observed in other areas of the NW Mediterranean Sea (Miquel et al., 1994). The very small net production (or consumption) of particles by planktonic communities described above indicates that these cannot play a significant role as sources of particles to support the substantial net transport of particles in the canyon. This, together with the high inorganic content of the particle flux, points to a dominant allochthonous and lithogenic nature of the particles transported in the canyon.

Because of downwelling flow, particles were probably transported near the bottom of the canyon, particularly in the central part of the canyon and nearshore where horizontal advection was reduced and retention time was higher. This may not apply to the offshore reaches of the canyon where advection actually increased as SW flow

meandered into the canyon. For these reasons, the canyon probably acted as a trap for those particles removed from the upper layer. Total particle transport includes the effects of particle sinking, as well as, hydrodynamic transport. A minimum sinking rate in the canyon can be estimated as the depth of the layer divided by the residence time in the layer. A conservative estimate of retention time is 6 d, based on a horizontal canyon velocity of 10 cm s^{-1} over a canyon reach of 24 km. For a particle sinking from the surface to the base of the lower layer we get a sinking speed of $200 \text{ m}/6 \text{ d} = 33 \text{ m d}^{-1}$. Phytoplankton have sinking rates of 1 m d^{-1} (Bienfang, 1980; Granata, 1991), $1\text{--}100 \text{ m d}^{-1}$ for organic aggregates and detritus (Alldredge and Silver, 1988), and $5\text{--}100 \text{ m d}^{-1}$ for other organic and inorganic particles (Mccave, 1975). Compared to the downwelling rate of nearly 40 m d^{-1} in the canyon, it is obvious that sedimentation is not important for transport of slower sinking particles; it may, however, be important for the deposition of faster sinking particles which can sink out before being advected out of the canyon. Another consideration is that particles sinking at lower rates might not be susceptible to transport out of the canyon area if they were trapped in the anticyclonic circulation cell. Upstream and offshore, where downwelling is weaker and horizontal advection is high, particles may simply be translated to other regions down the coast.

The transport rates presented in this paper should only be considered valid for the summer conditions which prevailed during this study since the reversal of flow on the shelf may not be an effect of the canyon itself. If the advection of low salinity water along the slope from the Gulf of Lions was the mechanism driving the flow reversal, as Rojas et al. (1995) have suggested, the flow pattern we found may be an episodic event. Flows along this coast are highly variable and dependent on the seasonal hydrological and meteorological conditions (Font et al., 1995). Alvarez et al. (1996) have demonstrated that, on time scales of 10 days, ageostrophic motions can cause significant changes in vertical velocities near the canyon head. Since our grid was sampled in 4 days, these motions may have been important; however, most of the evidence presented here shows that flow is geostrophic since density surfaces follow streamlines and streamlines display the same pattern as dynamics heights calculated with the CTD data (Rojas et al., 1995). On shorter time scales, motions such as tidal currents and internal waves are probably unimportant. In this part of the Mediterranean Sea tidal amplitudes are low and the influence of tidal currents are small (Alb erola et al., 1995). During our survey, an 8 hour time series of velocity from a station located in the canyon did not detect wave oscillations, but rather, indicated flow was eastward and relatively steady. Based on the above observations, it appears that flow is not ageostrophic and that our synoptic sampling did not seriously alias the flow/transport rates.

What is not clear from this study, however, is whether the material in the canyon is transported off the shelf or deposited on the canyon bottom. Examination of sedimentary fluxes and ^{210}Pb indicate that Mediterranean canyons play both these roles, as sediment depocenters and as conduits of particles to the deep basin (Monaco et al., 1990). All available evidence points, therefore, to a major role of canyons in the regulation of water flow, biological activity, and transport processes in the NW Mediterranean continental margin.

Acknowledgements

We wish to thank the crew and technical staff of the R/V *Hesperides* and the entire VARIMED group for their collaboration during data sampling. Special thanks to O. López and J. Sospedra, and P. Rojas from UPC who were involved in processing the raw CTD and ADCP data. This work was supported by grants AMB92-025a-C02-02, MAR93-0728, and AMB95-0437 from CICYT (Spanish Commission of Science and Technology). B. Vidondo was supported by a fellowship from the Spanish Ministry of Education and M.P. Satta by a grant from the Regione Autonoma della Sardegna. Lastly, we appreciate the comments of 3 anonymous reviewers whose suggestions greatly improved the manuscript.

References

- Albérola, C., Rousseau, S., Millot, C., Astraldi, M., Font, J., Garcia-ladona, E., Gasparini, G., Sent, U., Vangriesheim, A., 1995. Tidal currents in the Western Mediterranean sea, *Oceanologia Acta* 18, 273–284.
- Allredge, A.L., Silver, M.W., 1988. Characteristics, dynamics and significance of marine snow. *Progress in Oceanography* 20, 41–82.
- Alvarez, A., Tintoré, J., Sabatés, A., 1996. Flow modification and shelf-slope exchange induced by a submarine canyon off the northeast Spanish coast. *Journal of Geophysical Research* 101, 12,043–12,055.
- Bienfang, P.K., 1980. Phytoplankton sinking rates in the oligotrophic waters off Hawaii, USA. *Marine Biology* 61, 69–77.
- Carnevale, G.F., Purini, R., Briscolini, M., Vallis, G.K., 1989. Influence of topography on modon propagation and survival. In: Nihoul, J.C.J., Jamart, B.M. (Eds.), *Mesoscale/Synoptic Coherent Structures in Geophysical Turbulence*. Elsevier, Amsterdam, pp. 181–195.
- Castellón, A., Font, J., Garcia, E., 1990. The Liguro-Provençal-Catalan current (NW Mediterranean) observed by Doppler profiling in the Balearic Sea. *Scientia Marina* 54, 266–276.
- Demestre, M., Martin, P., 1993. Optimum exploitation of a demersal resource in the western Mediterranean: the fishery of the deep-water shrimp *Ariteus antennatus* (Risso, 1816). In: Leonart, J. (Ed.), *Northwestern Mediterranean Fisheries*. *Scientia Marina* 57, 175–182.
- Dickey, T., Siegel, D., 1988. A note on a control volume approach to vertical flux determinations in the upper ocean. Report of the U.S. GOFS, 3rd Pacific Planning Meeting, February 1988, U.S. GOFS WHOI, pp. 141–144.
- Durrieu de Madron, X., 1994. Hydrology and nepheloid structure in the Gran-Rhône canyon. *Continental Shelf Research* 14, 457–477.
- Fletcher, C.A.J., 1984. *Computational Galerkin Methods*, Springer, New York, 320 pp.
- Fofonoff, N.P., Millard, R.C., 1981. Algorithms for the computation of fundamental properties of seawater, UNESCO Tech. Paper 44, UNESCO, Paris, 160 pp.
- Font, J., Garcia-ladona, E., Gorriz, E.G., 1995. The seasonal variability of mesoscale motion in the Northern Current of the Western Mediterranean: several years of evidence. *Oceanologia Acta* 18, 207–220.
- Font, J., Salat, J., Tintoré, J., 1988. Permanent features of the circulation in the Catalan Sea, *Oceanologia Acta* SP, 51–57.
- Granata, T.C., 1991. Diel periodicity in growth and sinking rates of the centric diatom *Coscinodiscus concinnus*, *Limnology and Oceanography*, 36, 132–137.
- Hickey, B., Baker, E., Kachel, N., 1986. Suspended particle movement in and around the Quinault submarine canyon. *Marine Geology* 71, 35–83.
- Hockney, R., Eastwood, J., 1994. *Computer simulations using particles*. IOP Publications, London, 540 pp.
- Inman, D.L., Nordstron, C.E., Flick, R.E., 1976. Currents in submarine canyons: air-land-sea interaction. *Annual Review of Fluid Mechanics* 8, 275–310.

- Klinck, J.M., 1996. Circulation near submarine canyons: a modelling study. *Journal of Geophysical Research* 101, 1211–1223.
- Leach, H., 1987. The diagnosis of synoptic-scale vertical motion in the seasonal thermocline. *Deep-Sea Research* 34, 2005–2017.
- McCave, I.N., 1975. Vertical fluxes of particles in the ocean. *Deep-Sea Research* 22, 491–502.
- Masó, M., Tintoré, J., 1991. Variability of the shelf water off the northeast Spanish coast. *Journal of Marine Systems* 1, 441–450.
- Masó, M., Violette, P., Tintoré, J., 1990. Coastal flow modification by the submarine canyons along the NE Spanish coast. *Scientia Marina* 54, 343–348.
- Millot, C., 1990. The Gulf of Lions' hydrodynamics. *Continental Shelf Research* 10, 885–894.
- Miquel, J., Fowler, S., La Rosa, J., Brut-Menard, P., 1994. Dynamics of the downward flux of particles and carbon in the open northwestern Mediterranean Sea. *Deep-Sea Research I* 41, 243–261.
- Monaco, A., Courp, T., Heussner, S., Carbonne, J., Fowler, S.W., Deniaux, B., 1990. Seasonality and composition of particulate fluxes during ECOMARGE-I, western Gulf of Lions. *Continental Shelf Research* 10, 959–987.
- Olivar, M.P., Sabatés, A., Abelló, P., Garcia, M., 1998. Transitory hydrographic structures and distribution of fish larvae and neustonic crustaceans in the north-western Mediterranean. *Oceanologia Acta* 21, 95–104.
- Oudot, C., Gerard, R., Morin, P., Gningue, I., 1988. Precise shipboard determination of dissolved oxygen (Winkler procedure) for productivity studies with a commercial system. *Limnology and Oceanography* 33, 146–150.
- Rojas, P., García, M.A., Sospedra, J., Figa, J., Puig de Fabregas, J., Lopez, O., Espino, M., Ortiz, V., Sanchez-Arcilla, A., Manriquez, M., Shirasago, B., 1995. On the structure of the mean flow in the Blanes canyon area (NW Mediterranean) during summer. *Oceanologia Acta* 18, 443–458.
- Satta, M.P., Agustí, S., Mura, M.P., Duarte, C.M., 1996. Microplankton respiration and net community metabolism in the NW Mediterranean littoral. *Aquatic Microbial Ecology* 106, 165–172.
- Sabatés, A., Olivar, M.P., 1996. Variation of larval fish distributions associated with variability in the location of a shelf-slope front. *Marine Ecology Progress Series* 135, 11–20.
- Tintoré, J., Gomis, D., Alonso, S., Parrilla, G., 1991. Mesoscale dynamics and vertical motion in the Alborán Sea. *Journal of Physical Oceanography* 21, 811–823.
- Tintoré, J., Wang, D.-P., Violette, P.E., 1990. Eddies and thermohaline intrusions of the shelf/slope front off the Northeast Spanish coast. *Journal of Geophysical Research* 95, 1627–1634.
- Topping, J., 1971. *Errors of Observation and Their Treatment*. Chapman and Hall, London, 119 pp.
- Vollenweider, R.A., 1974. *A Manual on Methods for Measuring Primary Production in Aquatic Environments*. Blackwell Scientific Publications, New York, 213 pp.
- Williams, P.J. leB., Jenkinson, N.W., 1982. A transportable microprocessor-controlled Winkler titration suitable for field and shipboard use. *Limnology and Oceanography* 27, 576–684.